Patterning curved surfaces: Template generation by ion beam proximity lithography and relief transfer by step and flash imprint lithography

P. Ruchhoeft[a)]
Department of Electrical and Computer Engineering, University of Houston, Houston, Texas 77204

M. Colburn and B. Choi
Texas Materials Institute, The University of Texas at Austin, Austin, Texas 78712

H. Nounu
Department of Electrical and Computer Engineering, University of Houston, Houston, Texas 77204

S. Johnson, T. Bailey, S. Damle, M. Stewart, J. Ekerdt, and S. V. Sreenivasan
Texas Materials Institute, The University of Texas at Austin, Austin, Texas 78712

J. C. Wolfe
Department of Electrical and Computer Engineering, University of Houston, Houston, Texas 77204

C. G. Willson
Texas Materials Institute, The University of Texas at Austin, Austin, Texas 78712

(Received 2 June 1999; accepted 2 September 1999)

Submicron patterning of 1 in. diameter curved surfaces with a 46 mm radius of curvature has been demonstrated with step and flash imprint lithography (SFIL) using templates patterned by ion beam proximity printing (IBP). Concave and convex spherical quartz templates were coated with 700-nm-thick poly(methylmethacrylate) (PMMA) and patterned by step-and-repeat IBP. The developed resist features were etched into the quartz template and the remaining PMMA stripped. During SFIL, a low viscosity, photopolymerizable formulation containing organosilicon precursors was introduced into the gap between the etched template and a substrate coated with an organic transfer layer and exposed to ultraviolet illumination. The smallest features on the templates were faithfully replicated in the silylated layer. © *1999 American Vacuum Society.*
[S0734-211X(99)11006-0]

I. INTRODUCTION

There has been a growing interest in patterning of curved surfaces at submicron dimensions. Applications lie in the field of imaging technology, primarily in sensors and distortion free charge coupled device arrays, enabling simple, compact optical designs with ultrawide fields-of-view.[1] The patterning of curved samples on the 1 μm scale is a challenge because of the large depth of field that is needed for the topographical variation of the substrate. In this article we present two lithographic processes that successfully patterned curve surfaces: step and flash imprint lithography (SFIL)[2] and ion beam proximity printing (IBP).[3]

It has been demonstrated that compression molding processes are capable of producing 10 nm features in poly (methylmethacrylate) (PMMA) on flat substrates.[4–7] While these elegant techniques are well suited for specific applications, they may not provide a workable means to achieve layer-to-layer overlay at the dimensional tolerance required to fabricate advanced device structures. SFIL has been shown to imprint sub-100 nm features at room temperature at pressures below 15 psi and it has the added advantage of a transparent template through which a layer-to-layer alignment is feasible. We have sought to demonstrate a process that would enable low-cost generation of high-resolution features on curved substrates for use in fabrication of device structures that require accurate layer to layer registration.

The production of a curved SFIL template predicates the use of a lithography tool that can either directly write a pattern on the substrate or project a flat mask pattern onto the curved surface. The IBP technique employs a stencil mask illuminated by a broad beam of light ions. Large mask-to-wafer gaps can be employed if the ion beam is well collimated, making IBP ideally suited for patterning of difficult substrate topographies.

By combining IBP and SFIL, we were able to generate curved surface templates with high-resolution patterns and replicate their relief structures reliably and quickly on curved substrates.

II. PROCEDURE

Ion-beam exposures were carried out on a step-and-repeat proximity printer with an interferometrically controlled $X-Y$ stage that has been detailed previously.[2] Briefly, ions are generated in a duoplasmatron ion source (National Electrostatic Corporation, Inc., Madison, WI) and pass through a 10 m long beamline to the exposure station. A picoammeter measures the exposure current with a Faraday cup and integration software automatically controls the total exposure dose by actuating an electrostatic beam blanker.[8] The IBP

[a)]Electronic mail: Paul@bayou.uh.edu

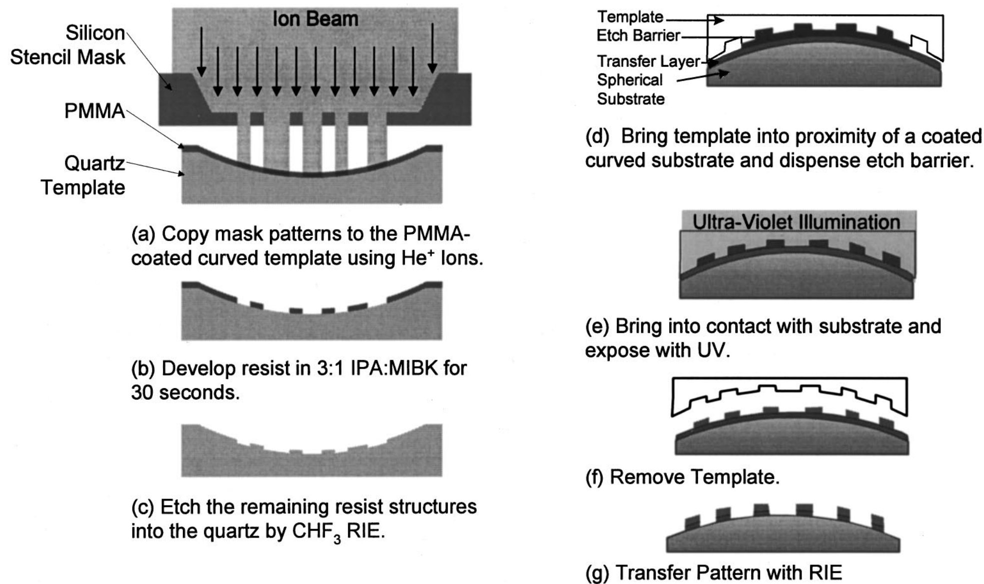

FIG. 1. Template and replica fabrication sequence.

masks were fabricated as described in Ref. 9 and consisted of various patterns etched through a 4-μm-thick silicon membrane.

The template manufacturing process is outlined in Figs. 1(a)–1(c). The template blanks were the concave portion of a quartz doublet, 2.5 cm in diameter with a 46 mm radius of curvature. A 700-nm-thick coating of PMMA (950 kg/mol) was applied to the blank by spin casting. After baking at 140° C for 30 min, the resist was exposed [Fig. 1(a)] with 150 keV He^+ ions and a dose of 3.0 μC/cm^2 and developed in a 3:1 mixture of isopropanol and methylisobutylketone for 30 s at room temperature. The mask-to-wafer gap varied between 4 and 9 mm over the sample. The PMMA pattern, thus formed [Fig. 1(b)], was transferred [Fig. 1(c)] into the quartz substrate by reactive ion etching (RIE) using CHF_3 chemistry in a homemade, magnetically enhanced reactor[9] at a pressure of 0.8 mTorr and 150 W of radio frequency power. The corresponding power density was about 0.25 W/cm^2 and the etch rates of both SiO_2 and PMMA were 25 nm/min. The total etch depth in the SiO_2 was about 0.2 μm. The remaining resist was removed by a low power O_2 RIE after quartz etching and the template surface treated as described previously.[1] We remark that no special procedures were used in spinning or etching to accommodate the curved substrate.

The collimation of the ion beam is a critical parameter that determines penumbral blur, and hence, resolution, and was measured for 75 keV He^+ ions by measuring the dependence of linewidth on dose. A mask with 0.8 μm wide lines was used with a mask-to-wafer gap of 1 cm. The substrates were silicon wafers coated with a 100-nm-thick layer of gold and a 50-nm-thick film of PMMA. Thin resist was used to ensure the accuracy of the threshold resist development model and gold was used on the substrates to enhance the secondary electron yield in the exposed areas, and thus, provide good contrast for measuring linewidth in a scanning electron microscope. The broad-area critical dose of the resist was determined by measuring dissolution rate versus dose with a 5 mm foil mask aperture, a diameter that is much larger than the blur. Collimation depends critically on the source parameters: in these experiments, the magnet current was zero, the extraction voltage was 30 keV and the arc voltage and current were 152 V and 0.5 A, respectively. A constant-gradient tube, also manufactured by NEC, accelerated the beam.

The replication of the template by SFIL is shown in Figs. 1(d)–1(g): (d) A 1.4 μm organic transfer layer was spin coated on a curved substrate. The curved template was closely aligned over the coated substrate and a drop of a low viscosity, photopolymerizable, organosilicon solution was introduced into the gap. The organosilicon solution, detailed previously, contains 47 wt % (acryloxypropyl) methylsiloxane–dimethylsiloxane copolymer, 3.5 wt % irgacure 184, 1.5 wt % irgacure 819 (Ciba), 24 wt % (3-acryloxypropyl)tris(trimethyl-siloxy)silane, and 24 wt % butyl acrylate.[2] The organosilicon fluid filled the gap by capillary action. (e) The gap was closed by vertical translation of the template toward the substrate until it made contact with the transfer layer. The structure was then irradiated with ultraviolet light through the backside of the template. (f) Once the photocuring was complete, the template was separated from the substrate leaving a relief image on the surface of the transfer layer. (g) An oxygen RIE through the transfer layer can be used to create a high aspect ratio image on the substrate. This entire process was conducted at room temperature, and, since the template is transparent, all of the alignment schemes that have been used successfully in mask aligners can, in principal, be implemented in a SFIL aligner.

An orientation stage was designed and fabricated for this imprint demonstration. Figure 2(a) shows two spherical surfaces, one representing the template and the other the substrate. These surfaces must have the same curvature. Two orientation schemes can yield surface-to-surface contact for

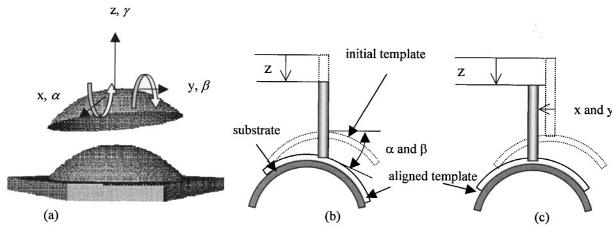

FIG. 2. (a) Two spherical surfaces representing a template and a substrate. (b) Alignment via one translation and two tilting motions. (c) Alignment via three translation motions.

TABLE I. Strain energy in distributed flexure stage.

Strain energy	Applied wrench
1.3125	15 lb force along x axis
1.3185	15 lb force along y axis
94.6136	15 lb force along z axis
119.0054	10 in.-lb torque about x axis
116.1306	10 in.-lb torque about y axis
1.4617	10 in.-lb torque about z axis

this case. The first is via one translation and two rotation motions. Figure 2(b) shows the initial and final states for two spherical surfaces oriented via this set of motions. The second scheme requires three translations ($x-y-z$ displacements). Figure 2(c) shows the orientation via three translations. Figure 3(a) shows an ideal stage composed of perfect rigid bodies and joints. Nonideal behavior, including distributed structural compliance, backlash, and stiction in joints etc., is neglected. Ideal kinematic stages provide insight into the geometry and force transmission at the template-substrate interface. This insight is then extended to the design of distributed flexure stages with selectively compliant and stiff directions. The connection from the base platform to the moving platform is via a combination of a revolute (R) joint, a prismatic (P) joint, and a ball (B) joint.

Sliding contacts in joints wear, generate particles and lead to stiction that makes precision control difficult. Flexures generate motion by elastic deformation and can avoid the problems associated with joints.[10] The major challenge with flexures is in designing mechanisms that provide the required motion-force characteristics. Figure 3(b) shows our flexure alignment stage design that is based on a ring comprised of three fixed–fixed beams.[11] The midpoint of each beam provides a vertical deflection in response to an applied vertical load. The three midpoints of the fixed–fixed beams are connected to the vacuum chuck that holds the wafer. Figure 3(c) illustrates the finite element model used to analyze the flexure stage. No linear or rotational displacement at the three locations where the flexure ring connects to the base is allowed. These conditions simulate a rigid structure supporting the flexure ring. Table I lists strain energies calculated from applied forces and displacements. For a given force (moment), the strain energy (or deflection) in x and y, and rotation about z are two orders of magnitude lower. Therefore, the stage allows rotations about x and y and translation in z while it has small translations in x and y and rotation about z. The distributed flexure stage exhibits exactly those motions desired for the substrate orientation stage.

III. RESULTS AND DISCUSSION

Excellent beam collimation in the IBP process is required to print submicron features over a substrate with extreme topography variation. So, collimation was measured for a 75 keV He^+ ion beam with a 1 cm mask-to-wafer gap and the source conditions described earlier. Figure 4(a) shows linewidth and exposure latitude versus dose for a 0.8 μm wide line in the mask. Here, exposure latitude is defined for a given dose as the maximum percentage that the dose can vary while keeping the linewidth change smaller than $\pm 10\%$ and was determined from a quadratic fit to the linewidth data. The exposure latitude is greater than 20% for the nominal (mask) linewidth of 0.8 μm.

The limited collimation of the beam introduces penumbral blur during the transfer of the mask pattern to the wafer. We model the blur with a Gaussian distribution, characterized by its full width at half maximum (FWHM). The spatial distribution of ion current on the substrate is obtained by convolving the mask pattern with the blur function. The FWHM of the Gaussian can be inferred from the dependence of linewidth on dose. Monte Carlo simulations using SRIM 2000[12] show the energy distribution to be extremely uniform with depth in thin resist (≤ 50 nm) and the micron-scale features to be more than two orders of magnitude larger than the extent of lateral scattering. We therefore expect the threshold model to describe resist development very accurately. In the

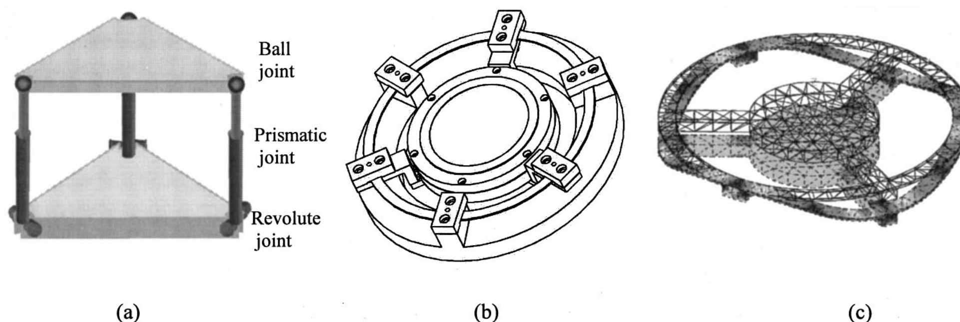

FIG. 3. (a) Ideal 3 degree-of-freedom stage, (b) distributed flexure design, and (c) deflected finite element model.

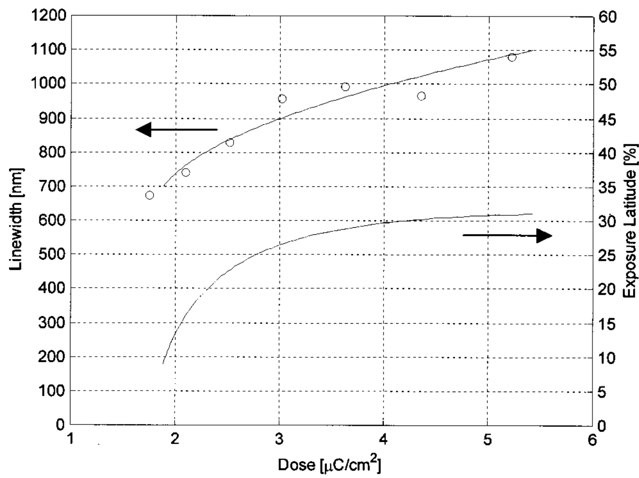

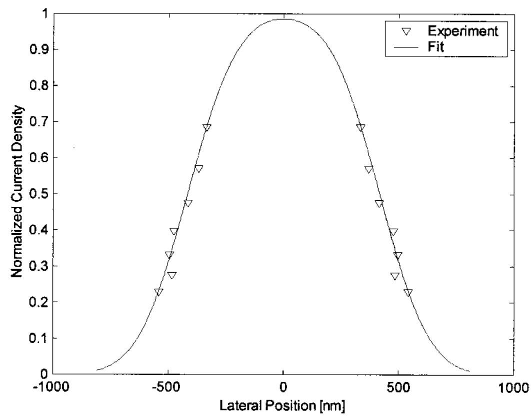

FIG. 4. (a) Linewidth and exposure latitude vs dose for 800 nm feature printed with 75 keV He^+ ions using a 1 cm mask-to-wafer gap. Exposure latitude is defined as percent change in dose for a 10% change in linewidth. (b) Normalized current density at the substrate: threshold approximation (line) with a 400 nm blur (FWHM) and the data (triangles) from (a).

threshold model, resist is assumed to be developed if the local dose is greater than D_0, the dose required to clear large areas, and to be undeveloped if the local dose is less. Our measurements, described earlier, showed $D_0 = 2.0$ μC/cm^2 for a 75 keV He^+ beam and 50-nm-thick PMMA. Now suppose that a dose D at the mask produces a line of width W at the wafer. Then, in the threshold model, the charge density at the line edge must be D_0, a fraction D_0/D of the dose incident on the mask. The linewidth/dose data can be easily transformed to linewidth versus D_0/D, and the best fit FWHM determined by a least square procedure. Figure 4(b) shows the fractional dose D_0/D versus position obtained from the experimental data in Fig. 4(a), together with the corresponding calculated values for a gaussian blur with a FWHM of 350 nm, the optimal value. This means, since the mask-to-wafer gap is 1 cm, that the collimation angle is 35 μrad (FWHM). Modeling shows that 0.5 μm features can be printed over 1 cm topography with a 10% exposure latitude at this voltage (75 keV). Even smaller features should be possible with the 150 keV beam that was used to print the template reported below. Figure 5 shows a 1.2 μm wide

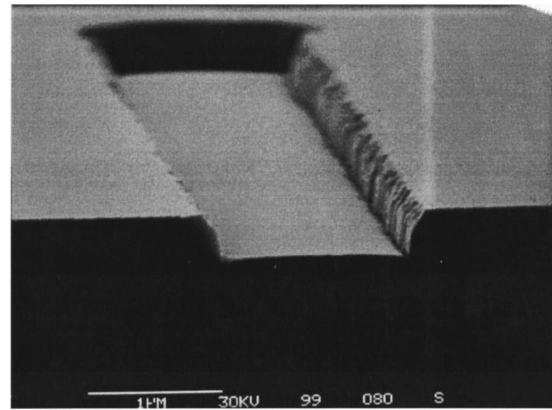

FIG. 5. 1.2 μm wide trench in SiO_2 printed with a 1 cm mask-to-wafer gap and etched with CHF_3 RIE.

trench in SiO_2 printed with a 1 cm mask-to-wafer gap and etched as discussed earlier. Radial pattern distortion due to local slope variations on the curved surface was not addressed in this work. However, uniform linewidth formation over the entire substrate can be achieved by predistorting the original mask pattern.

SFIL has demonstrated high fidelity replication of sub-100 nm features on flat substrates. The resolution of this process appears to be template limited. Extending the SFIL

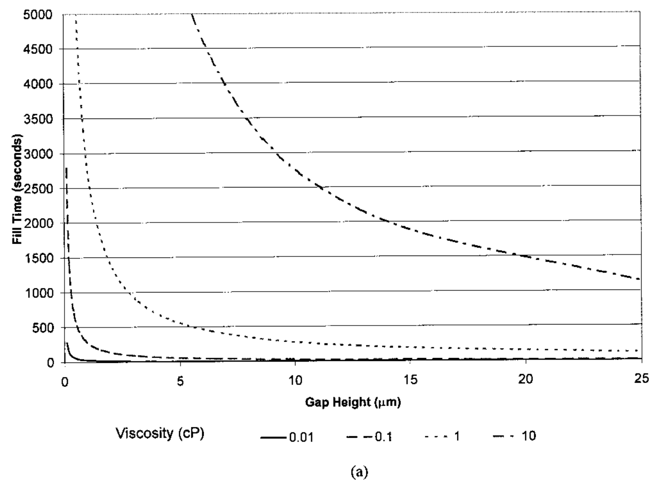

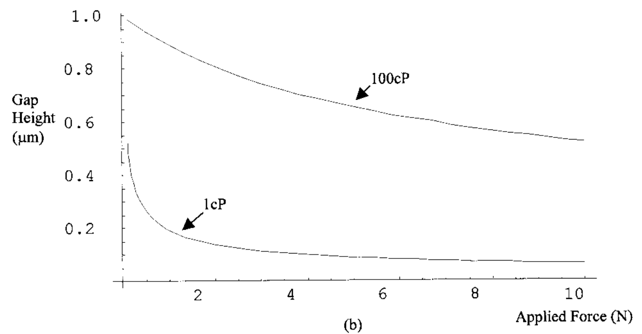

FIG. 6. (a) Capillary fill time as a function of gap height and viscosity. (b) Gap as a function of a 1 s applied force for different viscosities (1 and 100 cP). The contact area is π cm^2.

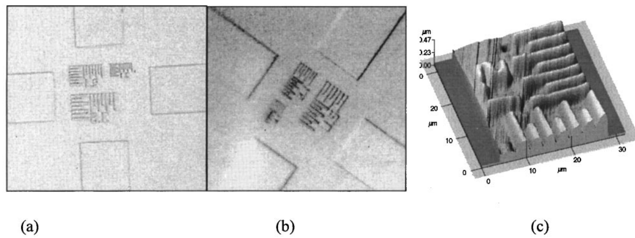

FIG. 7. (a) Optical micrograph shows features etched into the template generated by ion-proximity lithography. (b) Optical micrograph shows a relief pattern in the etch barrier. (c) AFM image of topography patterned in etch barrier.

process to curved substrates simply required a curved template and an appropriate stage. During the SFIL process, the gap between the substrate and the template is filled by capillary action. The rate at which the fluid fills the gap is described by the Washburn Eq. (1). The fill rate is proportional to H, the gap height, and γ_a, the surface tension. It is inversely proportional to R, the radius of curvature of the meniscus, and x, the distance of the meniscus along the length of the capillary.

$$\frac{dx}{dt}=\frac{(H^2\gamma_a/R)}{24\mu x}. \quad (1)$$

Figure 6(a) shows that for reasonable fill times, the gap must be larger than 10 μm. Filling such a large gap necessitates expelling large amounts of fluid into the kerf. If the gap is thin enough to avoid expelling excessive fluid in the kerf, it cannot be filled by capillary action in a reasonable time. Therefore, before the gap is filled completely by capillary action, we displace some fluid by a final translation of the template.

The pressure required to press two plates of radius, R, together through a liquid of viscosity μ, at a rate, V, and gap height, H, is given by Eq. (2). As illustrated in Fig. 6(b), rapid displacement is possible at low pressure with low viscosity solutions. Higher viscosity fluids (i.e., polymers) require much higher pressures to achieve the same displacement.

$$P_{\text{applied}}=\frac{3\mu VR^2}{4H^3}. \quad (2)$$

The photopolymerization kinetics and fluid fill dynamics requirements pose a complication. The rate of fluid displacement is inversely proportional to the viscosity of the fluid. Typical photopolymer fluids contain a blend of functionalized oligomers and reactive diluents. The viscosity of the solution is a steep function of the oligomer concentration, and so, unfortunately, is the cure rate. There is therefore a balance between fill rate and cure speed that must be considered in material design.

We are able to imprint 0.5 μm features reliably on the curved surfaces with an exposure dose of 100 mJ/cm^2 and imprint force of 5 lb/in.^{2}. Figures 7(a) and 7(b) show optical micrographs comparing patterns on the template to relief patterns produced in the photopolymer and Fig. 7(c) shows an atomic force microscopy (AFM) of the relief pattern. The process has high resolution and high fidelity. We believe the smallest of structures generated in the template can be accurately replicated by SFIL on flat or curved configurations.

IV. CONCLUSIONS

IBP printing was used to generate curved templates with high-resolution patterns. The large depth of field of IBP allows for the printing of submicron structures over a 1 cm mask-to-wafer gap that cannot be patterned by conventional optical lithography. SFIL was used to replicate the template patterns on curved surfaces with high fidelity. The SFIL process was conducted at room temperature and required low pressures, while other compression imprinting techniques require high temperatures, high pressures, and long processing times. A prototype SFIl apparatus has been designed that incorporates a new stage that eliminates image shear during illumination and separation. The process has very high resolution and excellent pattern fidelity.

ACKNOWLEDGMENTS

The authors thank 3M and IBM-Burlington for technical consultation and generous gifts to the project. The authors appreciate the assistance of Rachael Mahaffy. The authors gratefully acknowledge the financial support of SRC (Contract No. 96-LC-460) and DARPA (Grant No. N66001-98-1-8914).

[1]W. Hamilton, Internal Report DARPA MLP Participants (1999).
[2]M. Colburn *et al.*, SPIE's 24th International Symposium Microlithography: Emerging Lithographic Technologies III, 14–19 March 1999.
[3]D. P. Stumbo, G. A. Damm, S. Sen, D. W. Engler, F-O. Fong, J. C. Wolfe, and James A. Oro, J. Vac. Sci. Technol. B **9**, 3597 (1991).
[4]S. Y. Chou, P. R. Krauss, and P. J. Renstrom, J. Vac. Sci. Technol. B **14**, 4129 (1996).
[5]Y. Xia and G. M. Whitesides, Angew. Chem. Int. Ed. Engl. **37**, 550 (1998).
[6]J. Haisma, M. Verheijen, K. van der Huevel, and J. van den Berg, J. Vac. Sci. Technol. B **14**, 4124 (1996).
[7]H.-C. Scheer, H. Schults, F. Gottschalch, T. Hoffmann, and C. M. Torres, J. Vac. Sci. Technol. B **16**, 3917 (1998).
[8]J. C. Wolfe, S. V. Pendharkar, P. Ruchhoeft, S. Sen, M. D. Morgan, W. E. Horne, R. C. Tiberio, and J. N. Randall, J. Vac. Sci. Technol. B **14**, 3896 (1996).
[9]S. V. Pendarkar *et al.*, J. Vac. Sci. Technol. B **13**, 2588 (1995).
[10]S. Smith and D. G. Chetwynd, *Foundations of Ultraprecision Mechanism Design* (Gordon and Breach, Philadelphia, 1992).
[11]S. Johnson, M.S. thesis, The University of Texas at Austin, 1999.
[12]J. F. Ziegler, J. P. Biersack, and U. Littmark, *The Stopping and Ranges of Ions in Solids* (Pergamon, New York, 1985). Updated software (version of SRIM 2000) is found at http://www.research.ibm.com/ionbeams/